

Synthesis and NMR Studies of $[(C_5Me_5)Os(L)H_2(H_2)^+]$ Complexes. Evidence of the Adoption of Different Structures by a Dihydrogen Complex in Solution and the Solid State

Christopher L. Gross and Gregory S. Girolami*

The School of Chemical Sciences, The University of Illinois at Urbana-Champaign,
600 South Mathews Avenue, Urbana, Illinois 61801

Received November 5, 2006

Protonation of the osmium(IV) trihydrides $(C_5Me_5)OsH_3(L)$ with HBF_4 in diethyl ether affords the molecular dihydrogen complexes $[(C_5Me_5)Os(H_2)H_2(L)][BF_4]$, where L is PPh_3 (**1**), $AsPh_3$ (**2**), or PCy_3 (**3**). Ruthenium analogues of these species are not stable and instead lose H_2 readily. These compounds adopt four-legged piano-stool geometries in which the phosphine ligand is “trans” to an elongated dihydrogen ligand. For **1** and **2**, the coordinated H_2 ligand is oriented with its H–H vector nearly parallel with the Os–Ct vector, where Ct is the centroid of the C_5Me_5 ring; in contrast, in **3** the H_2 ligand is oriented with its H–H vector perpendicular to the Os–Ct vector. In the 1H NMR spectra, exchange between the Os–H and Os– H_2 environments can be slowed at low temperatures for the arsine complex **2** (but not for **1** or **3**), and separate resonances could be observed for the hydride and dihydrogen sites; the barrier for exchange is approximately 6.0 kcal/mol. Partially deuterated samples were prepared, and H–H distances within the bound H_2 ligands were deduced from the observed $^1J_{HD(av)}$ coupling constants. In addition, H–H distances were deduced from the $T_1(\text{min})$ values for the osmium-bound hydrogen atoms, after correction for exchange and ligand-induced dipolar relaxation effects. In all cases, the two solution measurements were in agreement but differed from that deduced from neutron diffraction data. Specifically, for **1** the solution data gave a distance of ca. 1.07 vs 1.01 Å in the solid state; similarly, for **2** the solution value of ca. 1.15 Å was longer than the 1.08 Å value seen in the solid state. In both cases, the ~ 0.06 Å lengthening in solution, if real, is the result most likely of one or both of two factors: the effect of removing the BF_4 counterion from the vicinity of the cation and the effect of librational motion that tends to shorten artificially H–H distances deduced from neutron diffraction data. In contrast, for **3** the solution H–H distance of ca. 1.12 Å is significantly shorter than the 1.31 Å distance determined from the neutron diffraction data. DFT calculations support the hypothesis that different structures are adopted by **3** in solution and in the solid state and that in solution an equilibrium is established between two dihydrogen–dihydride structures, one with a considerably shorter H–H bond than is seen in the solid state.

Introduction

The chemistry of metal hydrides has taken on renewed interest in the context of developing transportation systems in which hydrogen serves as the energy storage medium.^{1–5} One aspect of interest is how the structures and properties of transition-metal hydride complexes depend on the identity of the metal center. One trend is that the behavior of second- and third-row metal complexes is often rather different. For example, the second-row transition-metal complexes $(C_5H_5)_2NbH_3$ and $[(C_5H_5)_2MoH_3][BF_4]$ have classical polyhydride structures but exhibit pronounced quantum exchange with J_{HH} couplings as large as 1000 Hz.^{6–8} In contrast, the third-row analogues of these species, $(C_5H_5)_2TaH_3$ and $[(C_5H_5)_2WH_3][BF_4]$, exhibit classical behavior in their 1H NMR spectra.

Since their discovery, molecular dihydrogen complexes have generated considerable interest because they may represent a midway point along the reaction coordinate that leads to the oxidative addition of dihydrogen to transition-metal centers. The H–H bond distance is a measure of the extent to which the H_2 ligand has been activated. Distances less than 0.85 Å are typical for “normal” dihydrogen complexes, whereas distances longer than 1.50 Å are characteristic of classical dihydrides.⁹ A few dihydrogen complexes, however, have “elongated” H–H bond distances of approximately 1.0 to 1.4 Å that constitute an intermediate situation.⁴

We have recently described single-crystal neutron diffraction, inelastic neutron scattering, and density functional studies of the osmium complexes $[(C_5Me_5)OsH_4(L)][BF_4]$, where L = PPh_3 , $AsPh_3$, PCy_3 .¹⁰ All three compounds contain a dihydrogen ligand that falls into the “elongated” category. Interestingly, the structures of these complexes are not all the same: for the PPh_3

(1) Ogden, J. M. *Annu. Rev. Energy Environ.* **1999**, *24*, 227–279.
(2) Seayad, A. M.; Antonelli, D. M. *Adv. Mater.* **2004**, *16*, 765–777.
(3) Clapham, S. E.; Hadzovic, A.; Morris, R. H. *Coord. Chem. Rev.* **2004**, *248*, 2201–2237.
(4) Heinekey, D. M.; Lledos, A.; Lluch, J. M. *Chem. Soc. Rev.* **2004**, *33*, 175–182.
(5) Maseras, F.; Lledos, A.; Clot, E.; Eisenstein, O. *Chem. Rev.* **2000**, *100*, 601–636.
(6) Sabo-Etienne, S.; Chaudret, B. *Coord. Chem. Rev.* **1998**, *178*, 381–407.

(7) Heinekey, D. M. *J. Am. Chem. Soc.* **1991**, *113*, 6074–6077.
(8) Camanyes, S.; Maseras, F.; Moreno, M.; Lledós, A.; Lluch, J. M.; Bertrán, J. J. *J. Am. Chem. Soc.* **1996**, *118*, 4617–4621.
(9) Maseras, F.; Lledós, A.; Costas, M.; Poblet, J. M. *Organometallics* **1996**, *15*, 2947–2953.
(10) Webster, C. E.; Gross, C. L.; Young, D. M.; Girolami, G. S.; Schultz, A. J.; Hall, M. B.; Eckert, J. *J. Am. Chem. Soc.* **2005**, *127*, 15091–15101.

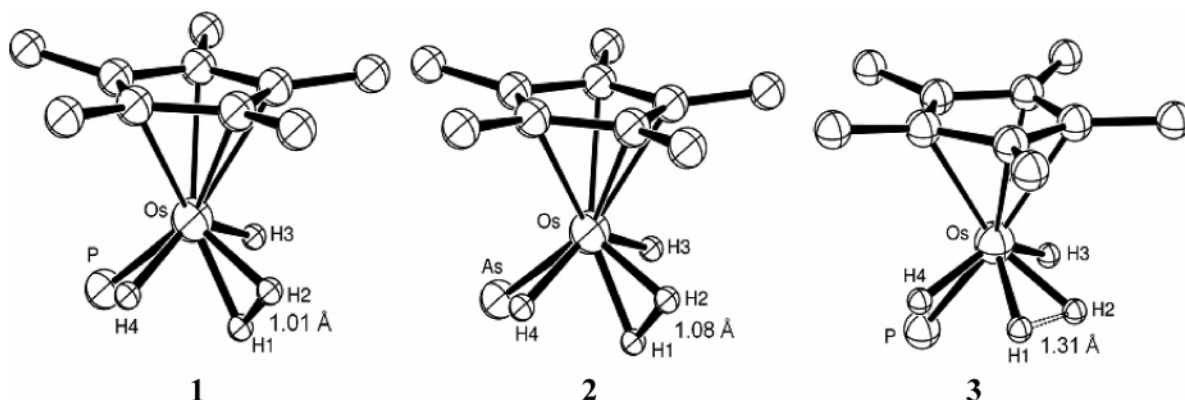


Figure 1. Inner coordination spheres of **1–3**. The phenyl and cyclohexyl groups bound to phosphorus and arsenic, and the methyl hydrogen atoms on the C₅Me₅ ligand, are omitted for clarity. Reproduced from ref 10.

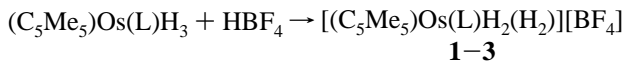
and AsPh₃ complexes, the coordinated H₂ ligand is oriented with its H–H vector approximately parallel with the Os–Ct vector, where Ct is the centroid of the C₅Me₅ ring; in contrast, for PCy₃ the H₂ ligand is oriented with its H–H vector perpendicular to the Os–Ct vector.

Density functional calculations showed that the molecular geometry is a consequence of a delicate balance of electronic and steric influences created by the L ligand. Highly important are steric interactions between the C₅Me₅ and L groups, which change the Ct–Os–L angle. The change in geometry changes the relative energies of the frontier orbitals that project toward the H₂ ligand; these frontier orbitals in turn govern the H–H distance, preferred H–H orientation, and rotational dynamics of the elongated dihydrogen ligand. The geometry of the dihydrogen ligand is further tuned by interactions with the BF₄[–] counterion.¹⁰

In order to complement the above solid-state studies, we now describe the synthesis and solution characterization of the [(C₅Me₅)Os(H₂(H₂L))⁺] complexes. A significant conclusion is that, for L = PCy₃, different structures are adopted in solution and the solid state. Portions of this work have been reported previously.¹¹

Results

Preparation of the Osmium Dihydrogen Complexes [(C₅Me₅)Os(L)H₂(H₂)⁺]. We have previously described the synthesis of a series of osmium(IV) trihydrides (C₅Me₅)Os(L)H₃, where L = PPh₃, AsPh₃, PCy₃.¹² These compounds adopt classical hydride structures in both solution and the solid state. Treatment of these species with HBF₄·Et₂O in diethyl ether generates products with the stoichiometry [(C₅Me₅)Os(L)H₄][BF₄], where L = PPh₃ (**1**), AsPh₃ (**2**), PCy₃ (**3**).



The compounds are isolated as white powders that precipitate from solution under the reaction conditions employed; recrystallization can be accomplished by layering concentrated CH₂Cl₂ solutions of the complexes with diethyl ether.

In a companion paper, we reported single-crystal neutron diffraction studies of **1–3**.¹⁰ Complementary information ob-

tained from X-ray crystallographic studies of the PPh₃ compound **1** and the PCy₃ compound **3** at 198 K can be found in the Supporting Information of the present article. In order to provide a context for the following NMR studies, we present only a summary of the structural details here, along with a brief description of how the molecular structure changes upon protonation.

All three compounds adopt four-legged piano-stool geometries in which the four legs are described by the Lewis base L, two classical hydride ligands, and a nonclassical dihydrogen ligand (Figure 1). The ligand L is “trans” to the dihydrogen ligand, and the two classical hydride ligands are “trans” to one another. For the PPh₃ and AsPh₃ complexes **1** and **2**, the H–H vector of the H₂ ligand lies parallel to the Ct–Os–L plane (Ct = centroid of the C₅Me₅ ring). In contrast, in the PCy₃ complex **3**, the H–H vector is perpendicular to the Ct–Os–L plane. Not only the orientation of the central two hydrogen atoms but also the H–H bond length between them depends significantly on the nature of L: the H···H distances determined from neutron diffraction are 1.01(1) and 1.08(1) Å for L = PPh₃, AsPh₃, respectively, but 1.31(3) Å for L = PCy₃. All of these H–H distances are characteristic of “elongated” dihydrogen ligands.^{13–17}

Protonation of the osmium(IV) trihydrides causes a change in the hybridization of the metal–ligand bonding orbitals, as shown by a comparison of the structure of the neutral trihydride (C₅Me₅)OsH₃(PPh₃)¹² with that of the tetrahydride cation **1**. The angle between the mutually “trans” terminal hydrides in the square base of the four-legged piano stool opens up considerably upon protonation from 119(2)° in (C₅Me₅)OsH₃(PPh₃)¹² to 132.6(5)° in **1**. In addition, the Os–P bond distance lengthens upon protonation from 2.263(1) Å in (C₅Me₅)OsH₃(PPh₃) to 2.338(1) Å in **1**. These geometrical changes are consistent with the presumably greater steric requirements of the dihydrogen ligand in **1** relative to the hydride ligand trans to the phosphine in (C₅Me₅)OsH₃(PPh₃). The geometric changes that take place

(13) Albinati, A.; Bakhmutov, V. I.; Caulton, K. G.; Clot, E.; Eckert, J.; Eisenstein, O.; Gusev, D. G.; Grushin, V. V.; Hauger, B. E.; Klooster, W. T.; Koetzle, T. F.; McMullan, R. K.; O’Loughlin, T. J.; Pélissier, M.; Ricci, J. S.; Sigalas, M. P.; Vymenits, A. B. *J. Am. Chem. Soc.* **1993**, *115*, 7300–7312.

(14) Klooster, W. T.; Koetzle, T. F.; Jia, G.; Fong, T. P.; Morris, R. H.; Albinati, A. *J. Am. Chem. Soc.* **1994**, *116*, 7677–7681.

(15) Maltby, P. A.; Schlaf, M.; Steinbeck, M.; Lough, A. J.; Morris, R. H.; Klooster, W. T.; Koetzle, T. F.; Srivastara, R. C. *J. Am. Chem. Soc.* **1996**, *118*, 5396–5407.

(16) Hasegawa, T.; Li, Z.; Parkin, S.; Hope, H.; McMullan, R. K.; Koetzle, T. F.; Taube, H. *J. Am. Chem. Soc.* **1994**, *116*, 4352–4356.

(17) Brammer, L.; Howard, J. A. K.; Johnson, O.; Koetzle, T. F.; Spencer, J. L.; Stringer, A. M. *J. Chem. Soc., Chem. Commun.* **1991**, 241–243.

(11) Gross, C. L.; Young, D. M.; Schultz, A. J.; Girolami, G. S. *J. Chem. Soc., Dalton Trans.* **1997**, *18*, 3081–3082.

(12) Gross, C. L.; Girolami, G. S. *Organometallics* **2006**, *25*, 4792–4798.

may also reflect changes in the energies of the frontier molecular orbitals upon protonation: these orbitals will decrease in energy upon protonation, owing to the addition of a positive charge and the ability of the H₂ ligand to act as a π -acceptor. Changes in the orbital makeup of the Os–H bonds may therefore be responsible for the increase in the trans H–Os–H angle, whereas a decrease in π -back-bonding to the PPh₃ ligand may explain the lengthening of the Os–P bond.

It is interesting to note that protonation of the analogous ruthenium trihydride complex (C₅Me₅)Ru(PPh₃)H₃ with HBF₄·Et₂O in toluene does not produce a product containing four metal-bound hydrogen ligands. Instead, a mixture of species is obtained that includes the dihydride cation [(C₅Me₅)Ru(PPh₃)₂H₂⁺] and the toluene π -complex [(C₅Me₅)Ru(η^6 -C₆H₅-Me)⁺].¹⁸ These products indicate that the initially produced [(C₅Me₅)Ru(PPh₃)H₄⁺] cation is unstable toward loss of H₂. The stability of [(C₅Me₅)Os(PPh₃)H₂(H₂)⁺] vs the ready loss of H₂ from its ruthenium analogue reflects the general trend that third-row transition metals form stronger metal–ligand bonds than do their second-row congeners.

Spectroscopic Characterization of the Osmium Dihydrogen Complexes. The infrared spectrum of the PPh₃ compound **1** exhibits two Os–H stretching bands at 2108 and 2063 cm⁻¹ with the higher frequency band at 2108 cm⁻¹ being the more intense of the two ($I_{2108}/I_{2063} = 1.9$). Most likely, these features are due to the Os–H stretching vibrations of the classical hydride ligands. The infrared spectrum of the AsPh₃ compound **2** contains two Os–H bands at 2088 and 2029 cm⁻¹ whose frequencies and intensities are similar to those seen for **1**. In contrast, the infrared spectrum of the PCy₃ compound **3** contains two bands in the Os–H stretching region at 2173 and 2102 cm⁻¹, with the lower frequency band being the more intense by about a factor of 2. These findings are consistent with the crystallographic results, which show that the structures of **1** and **2** are similar but fundamentally different from that of **3**.

The room-temperature ¹H NMR spectra of **1–3** in CD₂Cl₂ all feature a single resonance for the four osmium-bound hydrogen atoms; the resonances for the PPh₃ complex **1** and the PCy₃ complex **3** appear as doublets at δ -9.61 ($J_{\text{HP}}(\text{av}) = 14.2$ Hz) and δ -10.61 ($J_{\text{HP}}(\text{av}) = 15.7$ Hz), whereas the resonance for the AsPh₃ complex **2** is a singlet at δ -9.88. Thus, it is apparent that exchange of the classical and nonclassical hydrogen atom sites in compounds **1–3** is fast on the NMR time scale at 25 °C. The hydride resonances of **1** and **3** remain sharp down to approximately -100 °C, at which point they begin to broaden. Even at -140 °C (in the solvent CDFCl₂), however, the hydride resonances of **1** and **3** remain broad singlets. In contrast, the hydride resonance of **2** at -140 °C decoalesces into two broad equal-intensity features separated by 1.0 ppm (Figure 2). From this chemical shift separation and the coalescence temperature, we can calculate that the activation free energy for the dihydrogen/hydride exchange process in **2** is ~6.0 kcal/mol.

Additional insight into the solution structures can be obtained from the NMR spectra of partially deuterated isotopologues of **1** and **2**. Addition of a 3:1 mixture of D₂O and HBF₄·Et₂O to a diethyl ether solution of (C₅Me₅)OsD₃(PPh₃) generates a distribution of isotopologues of **1**, including [(C₅Me₅)Os(PPh₃-D₂(D₂)] [BF₄], the fully deuterated material. At 25 °C, the ¹H NMR resonance for the residual hydrogen atoms in the hydride sites is a doublet (${}^2J_{\text{HP}}(\text{av}) = 14.7$ Hz) of multiplets (Figure

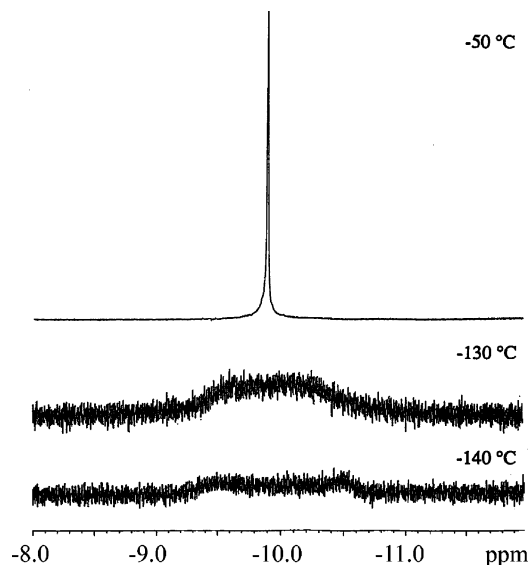


Figure 2. Hydride region of the 500 MHz ¹H NMR spectra of [(C₅Me₅)Os(AsPh₃)H₂(H₂)] [BF₄] (**2**) in CDFCl₂ at -50 °C (top), -130 °C (middle), and -140 °C (bottom).

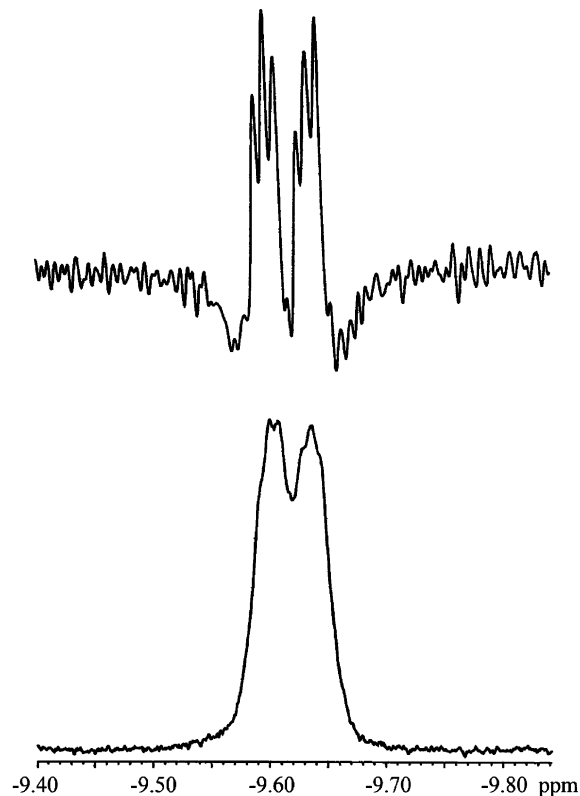


Figure 3. Hydride region of the 400 MHz ¹H NMR spectrum of [(C₅Me₅)Os(PPh₃)HD₃] [BF₄] (**1-d₃**) at 25 °C in CD₂Cl₂. The top spectrum is resolution enhanced. The doublet splitting is due to ³¹P; the 1:1:1 triplet splitting is due to ²H.

3); the multiplet splitting gives $J_{\text{HD}}(\text{av}) = 3.6$ Hz. These coupling constants are averages owing to the dynamic exchange process; if we assume that there is no site preference for the H and D atoms, the average coupling constant is equal to $[{}^1J_{\text{HD}} + 4({}^2J_{\text{HD}}) + {}^2J'_{\text{HD}}]/6$, where ${}^1J_{\text{HD}}$, ${}^2J_{\text{HD}}$, and ${}^2J'_{\text{HD}}$ are the couplings within the dihydrogen ligand, between the dihydrogen and hydride atoms, and between the two classical hydride atoms, respectively. If we adopt typical values for the geminal ${}^2J_{\text{HD}}$ couplings of between -1 and +1 Hz,^{19–24} then the intrinsic ${}^1J_{\text{HD}}$ coupling within the bound HD ligand is between 16.6 and

(18) Arliguie, T.; Chaudret, B.; Jalon, F. A.; Otero, A.; Lopez, J. A.; Lahoz, F. J. *Organometallics* **1991**, *10*, 1888–1896.

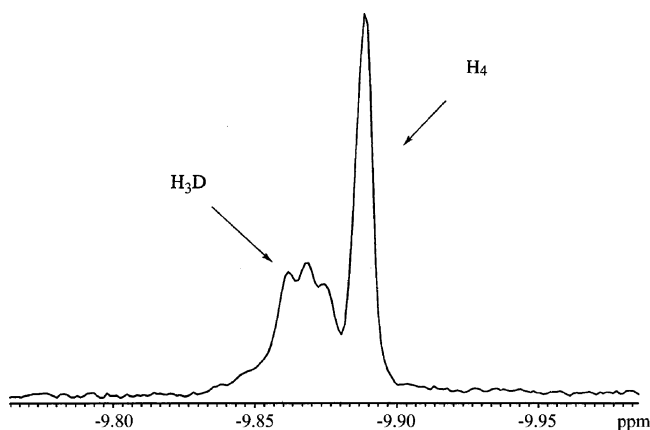


Figure 4. Hydride region of the 400 MHz ¹H NMR spectrum of a mixture of [(C₅Me₅)Os(AsPh₃)H₄][BF₄] and [(C₅Me₅)Os(AsPh₃)-H₃D][BF₄] (**2-d₀** and **2-d**) at 25 °C in CD₂Cl₂.

26.6 Hz. This span, when substituted into an expression that relates ¹J_{HD} to H–H distances,^{24,25} affords values of 0.97–1.18 Å, a range that includes the 1.01 Å value determined from the neutron diffraction study.¹⁰

In similar experiments, **2** and **3** were individually mixed with a small amount of trifluoromethanesulfonic acid-*d* in CD₂Cl₂. For **2**, the hydride region of the ¹H NMR spectrum of this mixture features a 1:1:1 triplet due to the monodeuterated isotopologue of **2** and a singlet due to the unlabeled compound (Figure 4). The multiplet splitting of the resonance for the labeled product affords a J_{HD(av)} value of 2.8 Hz. When it is treated as described above, the J_{HD(av)} value of 2.8 Hz gives an intrinsic ¹J_{HD} coupling of between 11.8 and 21.8 Hz and distances of 1.06–1.32 Å for the H–H ligand, a range that once again includes the 1.07 Å value established from the neutron diffraction study.

For deuterated samples of **3**, the hydride region of the ¹H NMR spectrum contains a number of overlapping doublets of multiplets due to the presence of several isotopologues. The multiplet splitting affords a J_{HD(av)} value of 3.4 Hz, which, in turn, gives an intrinsic ¹J_{HD} coupling of between 15.4 and 25.4 Hz and H–H distances of 0.99–1.21 Å (vs 1.31 Å from the neutron diffraction study). For **3**, the experimental H–H distance falls outside the range estimated from the solution data.

It is clear from the above results that uncertainties in the values of the two-bond J_{HD} coupling constants (i.e., those involving the classical hydrides) make it difficult to derive accurate H–H bond distances for polyhydrides in which exchange between the classical and nonclassical hydride sites is fast on the NMR time scale. Nevertheless, we can conclude that for **1** and **2** the H–H distance calculated from the average

J_{HD} coupling constant is consistent with the solid-state results, whereas for the PCy₃ compound **3** the results are inconsistent with the solid-state structure.

For undeuterated samples of **1–3**, we have also carried out variable-temperature ¹H NMR studies of the spin–lattice relaxation time, a parameter that also can provide information about the H–H distance.^{26–29} At 500 MHz in CD₂Cl₂, the T_{1(av, min)} values of the Os–H resonances are 99 ms (at –70 °C), 130 ms (at –70 °C), and 41 ms (at –90 °C) for **1–3**, respectively. At these temperatures, the exchange between the Os–H and Os–H₂ sites is in the fast exchange limit, and thus the observed relaxation time is an average given by the expression R(av, min) = 1/2[R(c, min) + R(n, min)], where R(c, min) and R(n, min) are the relaxation rates (R = 1/T₁) for the classical and nonclassical hydrogen sites at the T_{1(av, min)} temperature.

Because all three compounds **1–3** have been characterized by neutron diffraction, we can use Halpern's method^{27,28} to calculate R(c, min) values for each of the two classical hydride atoms; this parameter should be equal to the sum of the dipole–dipole relaxation contributions from all the other nuclear spins in the molecule (correcting for the natural abundance where necessary). The dipole–dipole relaxation contributions can be calculated from the experimentally determined H···X distances between the hydrogen atom of interest and all of the other atoms in the molecule. From the calculated value of R(c, min) and the experimental value of R(av, min), we can calculate R(n, min) from the formula above. After correcting the latter value for the dipole–dipole relaxations induced by nearby atoms *except* that due to the mutual action of the two hydrogen atoms in the H₂ molecule, we can use established formulas to deduce the value of d_{HH} within the H₂ ligand.^{26–29} If the resulting H–H distance within the H₂ ligand is similar to that in the solid state, then it is reasonable to conclude that the solution and solid-state structures are similar. If, however, this procedure gives a H–H distance significantly different from that in the solid state, then one can conclude that the solution and solid-state structures are different.

From the experimental H···X distances between each of the two classical hydrogen atoms in **1** and the other nuclear spins (¹H, ³¹P, ¹⁸⁷Os), we can calculate that R(c, min) should be 4.14 s^{–1}. This rate, combined with the 99 ms value of T_{1(av, min)}, leads to an estimated value of 16.1 s^{–1} for R(n, min). Subtracting out the dipole–dipole relaxation rates due to the other nuclear spins (i.e. excluding the two H atoms within the H₂ ligand) affords a value of 13.0 s^{–1} (i.e. T_{1(n, min)} = 77 ms). This value should be the relaxation rate due just to the dipole–dipole interaction within the H₂ ligand. If we assume that the dihydrogen ligand rotation rate is fast compared with the molecular tumbling rate, then from the expression d_{HH} = 5.81 · (T_{1(n, min)/4ν)^{1/6}, where the distance is expressed in Å, T₁ is in seconds, and ν is the spectrometer frequency in MHz,^{26–29} we obtain d_{HH} = 1.07 Å, vs 1.01 Å from the neutron diffraction study.¹⁰ The assumption that the H₂ rotation rate is fast compared with the molecular tumbling rate is consistent with the small rotational barrier of the bound H₂ ligand in [(C₅Me₅)OsH₄(PPh₃)⁺], the experimental value being 3.1 kcal mol^{–1}, as determined from inelastic neutron scattering experiments.¹⁰}

(26) Morris, R. H. *Can. J. Chem.* **1996**, *74*, 1907–1915.

(27) Desrosiers, P. J.; Cai, L.; Lin, Z.; Richards, R.; Halpern, J. J. *Am. Chem. Soc.* **1991**, *113*, 4173–4184.

(28) Bayse, C. A.; Luck, R. L.; Schelter, E. J. *Inorg. Chem.* **2001**, *40*, 3463–3467.

(29) See: Gusev, D. G.; Kuhlman, R. L.; Renkema, K. B.; Eisenstein, O.; Caulton, K. G. *Inorg. Chem.* **1996**, *35*, 6775–6783 and references therein.

(19) An upper limit on the magnitude of the two-bond ²J_{HH} coupling constant between mutually *cis* classical hydrides is 6 Hz (trans couplings can be as large as 15 Hz).^{20–24} Correcting for the H/D gyromagnetic ratio of 6.51 gives a maximum ²J_{HD} coupling constant between *cis* classical hydrides of about 1 Hz. Interestingly, it is thought that the sign of this coupling constant is negative.²⁴

(20) Herrmann, W. A.; Okuda, J. *Angew. Chem., Int. Ed. Engl.* **1986**, *25*, 1092–1093.

(21) Lantero, D. R.; Motry, D. H.; Ward, D. L.; Smith, M. L., III. *J. Am. Chem. Soc.* **1994**, *116*, 10811–10812.

(22) Ditzel, E. J.; Robertson, G. B. *Aust. J. Chem.* **1995**, *48*, 1183–1191.

(23) Delpuch, F.; Sabo-Etienne, S.; Donnadiou, B.; Chaudret, B. *Organometallics* **1998**, *17*, 4926–4928.

(24) Gründemann, S.; Limbach, H.-H.; Buntkowsky, G.; Sabo-Etienne, S.; Chaudret, B. *J. Phys. Chem. A* **1999**, *103*, 4752–4754.

(25) Gelabert, R.; Moreno, M.; Lluch, J. M.; Lledos, A.; Pons, V.; Heinekey, D. M. *J. Am. Chem. Soc.* **2004**, *126*, 8813–8822.

Table 1. H–H Distances (Å) for [(C₅Me₅)Os(L)H₂(H₂)] [BF₄] Complexes Determined by Different Methods

method	L		
	PPh ₃ (1)	AsPh ₃ (2)	PCy ₃ (3)
neutron diff ^a	1.01(1)	1.08(1)	1.31(3)
X-ray diff	0.78(8)	not detd	1.14(7)
<i>J</i> _{HD} ^b	0.97–1.18	1.06–1.32	0.99–1.21
<i>T</i> ₁ (min)	1.07 ^c	1.15 ^c	1.12 ^d

^a From ref 10. ^b The range corresponds to varying the ²*J*_{HD} coupling constants involving the classical hydride ligands between –1 and +1 Hz. ^c Fast rotation assumption. ^d Slow rotation assumption.

A similar analysis has been applied to the *T*₁ data for the AsPh₃ compound **2**. If we assume that the H₂ ligand is in the fast rotation limit, this procedure affords a value of 1.15 Å for the H–H distance in **2**, vs 1.08 Å for from the neutron diffraction study. Thus, for both **1** and **2**, the H–H distance derived from the relaxation data is slightly longer than the distance seen in the solid state.

For the PCy₃ compound **3**, by following the same procedure as that above and applying the fast-rotation assumption, we obtain a calculated H–H distance of 0.89 Å for the dihydrogen ligand in **3**. If we assume instead that the H₂ ligand in **3** is in the slow rotation limit, then we calculate a value of 1.12 Å for the H–H distance. Both values differ considerably from the neutron diffraction value of 1.35 Å, and this finding strongly supports the conclusion from the *J*_{HD} data that the solution structure differs from the solid-state structure.

Esteruelas has recently described the preparation of a similar dihydride-elongated dihydrogen derivative, [(C₅H₅)Os(PⁱPr₃)H₂(H₂)⁺], as both the BF₄ and triflate salts.³⁰ The average *J*_{HP} coupling constant of 14.1 Hz is very similar to the value we observe for **1**. The *T*₁ value decreases from 950 ± 20 ms at 0 °C to 106 ± 1 ms at –93 °C but did not reach a minimum in this temperature range. Partial deuteration afforded an average *J*_{HD} coupling constant of 3.6 Hz, corresponding to a H–H distance of about 1.1 Å, which agrees well with that found in **1** by neutron diffraction.

Comparison of H–H Distances Determined by Different Methods. Table 1 summarizes the H–H distances derived from neutron diffraction, X-ray diffraction, H–D coupling constants, and variable-temperature proton relaxation rates. In making these comparisons, it should be kept in mind that neutron diffraction data are collected at 20 K, vs ~200 K for the *J*_{HD}(av) and *T*₁(min) measurements. Because the H–H distances derived from the average H–D coupling constants are especially uncertain, owing to the unknown values of the intrinsic two-bond coupling constants involving the classical hydride ligands, we will focus our discussion on the distances determined from the relaxation experiments. Similarly, the H–H distances determined from the X-ray studies are highly uncertain and we will instead focus on the neutron diffraction results.

One principal conclusion of this work is that the H–H bond distances for **1** and **2** determined from the *T*₁(min) measurements are both ca. 0.06 Å longer than the values obtained by neutron diffraction. The difference may be ascribable in part to the effects of librational motion on the H–H distance derived from neutron diffraction: such motion artificially shortens the H–H bond distance by 0.02–0.1 Å.^{14,31} Another explanation of the longer H–H distances deduced in the solution experiments can

be derived from DFT calculations on **1** and **2**.¹⁰ When the BF₄ counterion is included in the calculations (as a gas-phase ion pair; i.e., in the absence of solvent), there is a single, minimum energy structure (containing one dihydrogen ligand) that is very similar to that determined by neutron diffraction. Interestingly, when the BF₄ counterion is removed and the structure of the free cation optimized, there are two principal low-energy structures of approximately equal energy: the observed dihydride–dihydrogen structure is slightly lower in energy than a tetrahydride isomer by 0.17 kcal mol^{–1}. Removal of the BF₄ counterion increases the optimized H–H distance in the dihydride–dihydrogen structure by approximately 0.1 Å. Thus, the DFT calculations present two possibilities for why the H–H distance is longer in solution: the H–H distance in the dihydrogen ligand increases when the BF₄ counterion is removed from the vicinity of the cation, and another structure with four classical hydride ligands becomes similar in energy to the dihydride–dihydrogen structure. Thus, the theoretical results are consistent with the present solution experiments, which suggest that the H–H distance is longer in solution than in the solid state.

For the PCy₃ compound **3**, the *T*₁(min) value affords a H–H distance of 0.89 Å if we assume that the H₂ ligand is rotating rapidly relative to the molecular tumbling rate in solution but 1.12 Å if we assume that rotation is slow. The former value is unlikely, in view of the DFT calculations (see below); thus, **3** differs from **1** and **2** in that the rate of H₂ rotation is slow rather than fast relative to the rate of molecular tumbling. The reason for this difference in rotation rates may be related to the electronic factors responsible for the different structure adopted by **3** in the solid state; perhaps also relevant is the proposal that cis dihydride–dihydrogen interactions can affect the barrier to H₂ rotation.^{32,33}

Unlike the behavior seen for **1** and **2**, in which the solution H–H distances are *longer* than that deduced by neutron diffraction by about 0.06 Å, for **3** the solution H–H distances are *shorter* by about 0.15 Å. DFT calculations again afford some insight into this finding.¹⁰ When the BF₄ counterion is included in the calculations, there is a single minimum-energy structure in which the two central hydrogens form a very elongated H₂ ligand (H–H = 1.51 Å) oriented with the H–H vector, as seen in the solid state (perpendicular to the Ct–Os–L plane). For the free cation, the DFT calculations reveal that there are multiple minima. Significantly, in one of them, which lies only 1.5 kcal mol^{–1} above the global minimum, the H–H vector is still perpendicular to the Ct–Os–L plane but the H···H distance of 1.10 Å is much shorter than that in the global minimum structure. We suggest that this structure is present in solution, perhaps in equilibrium with the structure with the longer H–H bond, and is responsible for the shorter H–H distance deduced from the solution NMR data. It is unlikely that the different H–H distance deduced from the relaxation data is due to changes in the conformation of the cyclohexyl rings of the PCy₃ ligand, because these atoms contribute relatively little to the dipole–dipole relaxation rates.

Few other examples of polyhydrides are known that adopt more than one structure in solution or that adopt different structures in solution vs the solid state.³⁴ The molecule

(32) Eisenstein, O.; Jackson, S. A. *Inorg. Chem.* **1990**, *29*, 3910–3914.

(33) Bianchini, C.; Masi, D.; Perruzzini, M.; Casarin, M.; Maccato, C.; Rizzi, G. A. *Inorg. Chem.* **1997**, *36*, 1061–1069.

(34) We exclude from consideration polyhydrides in which a single ground-state structure is dynamic via a high-energy intermediate and instead restrict our discussion to structures that have non-negligible populations at equilibrium.

(30) Esteruelas, M. A.; Hernandez, Y. A.; Lopez, A. M.; Olivan, M.; Onate, E. *Organometallics* **2005**, *24*, 5989–6000.

(31) Kubas, G. J.; Burns, C. J.; Eckert, J.; Johnson, S. W.; Larson, A. C.; Vergamini, P. J.; Unkefer, C. J.; Khalsa, G. R. K.; Jackson, S. A.; Eisenstein, O. *J. Am. Chem. Soc.* **1993**, *115*, 569–581.

[ReH₄(CO)(PMe₂Ph)₃]⁺ exists in solution as a mixture of the dihydrogen–dihydride and classical tetrahydride forms,^{35–37} a finding that has been supported by DFT calculations.^{38,39} Gusev⁴⁰ has shown that [FeH₃(PMe₃)₄]⁺ and [RuH₃(PEt₃)₄]⁺ isomerize between six-coordinate M^{II} dihydrogen–hydride and seven-coordinate M^{IV} trihydride geometries, and similar systems have been studied theoretically.⁴¹

Experimental Section

All operations were carried out under argon or vacuum by using standard Schlenk techniques. Solvents were distilled under nitrogen from sodium benzophenone (diethyl ether, pentane) or magnesium (ethanol). The osmium compounds (C₅Me₅)Os(L)H₃ were synthesized as described elsewhere.¹² Tetrafluoroboric acid (Aldrich) and deuterium oxide (Cambridge) were used without further purification.

Elemental analyses were performed by the University of Illinois Microanalytical Laboratory. Field desorption mass spectra were recorded on a Finnigan-MAT 731 mass spectrometer from samples loaded as solutions in dichloromethane. The IR spectra were recorded on a Perkin-Elmer 1700 FT-IR instrument as Nujol mulls between KBr plates. The ¹H and ³¹P NMR data were recorded on a Varian Unity 400 spectrometer at 400 and 161 MHz, respectively; ¹³C NMR spectra were recorded on a Varian Unity 500 spectrometer at 101 MHz. Some NMR spectra were recorded on General Electric QE-300, GN-300, and GN-500 instruments. Chemical shifts are reported in δ units (positive shifts to high frequency) relative to SiMe₄ (¹H and ¹³C) or H₃PO₄ (³¹P). T₁ measurements were made by the inversion recovery method, with the time-dependent intensities fitted by least squares to an exponential formula.

(Pentamethylcyclopentadienyl)dihydrido(η²-dihydrogen)(triphenylphosphine)osmium(IV) Tetrafluoroborate, [(C₅Me₅)Os-(PPh₃)H₂(H₂)] [BF₄] (1). To a solution of (C₅Me₅)OsH₃(PPh₃) (0.45 g, 0.76 mmol) in diethyl ether (25 mL) was added HBF₄·Et₂O (0.20 mL, 2.7 mmol). A white precipitate formed immediately. The solution was stirred at room temperature for 1.5 h, and the white solid was collected by filtration. Yield: 0.48 g (93%). Anal. Calcd for C₂₈H₃₄BF₄OsP: C, 49.6; H, 5.05; P, 4.56. Found: C, 49.6; H, 5.05; P, 4.27. ¹H NMR (CD₂Cl₂): δ 7.52 (m, *m*-CH + *p*-CH, 9H), 7.34 (m, *o*-CH, 6H), 2.06 (d, J_{PH} = 1.4 Hz, C₅Me₅, 15H), -9.62 (d, J_{PH} = 14.2 Hz, Os-H, 4H). ¹³C{¹H} NMR (CD₂Cl₂): δ 133.2 (d, J_{PC} = 62.6 Hz, *i*-C), 133.1 (d, J_{PC} = 10.7 Hz, *o*-C), 132.1 (d, J_{PC} = 3.1 Hz, *p*-C), 129.3 (d, J_{PC} = 11.4 Hz, *m*-C), 100.4 (s, C₅Me₅), 10.8 (s, C₅Me₅). ³¹P{¹H} NMR (CD₂Cl₂): δ 10.9 (s). IR (Nujol, cm⁻¹): 2108 (m), 2063 (m), 2008 (w), 1979 (w), 1822 (w), 1586 (w), 1578 (w), 1483 (s), 1436 (s), 1342 (w), 1334 (w), 1313 (m), 1284 (m), 1181 (w), 1163 (m), 1094 (s), 1062 (s), 1051 (s), 1036 (s), 1027 (s), 1006 (m), 997 (m), 977 (w), 965 (w), 934 (w), 920 (w), 894 (w), 856 (w), 834 (w), 786 (m), 757 (m), 752 (m), 747 (s), 697 (s), 593 (w), 533 (s), 519 (m), 511 (s), 503 (s), 467 (m), 434 (w), 426 (w).

(Pentamethylcyclopentadienyl)dihydrido(η²-dihydrogen)(triphenylarsine)osmium(IV) Tetrafluoroborate, [(C₅Me₅)Os(AsPh₃)H₂(H₂)] [BF₄] (2). To a solution of (C₅Me₅)OsH₃(AsPh₃) (0.15 g, 0.24 mmol) in diethyl ether (15 mL) was added HBF₄·Et₂O (0.10 mL, 1.3 mmol). A white precipitate formed immediately. The solution was stirred at room temperature for 20 min, and the white

solid was collected by filtration. Yield: 0.14 g (81%). Anal. Calcd for C₂₈H₃₄BF₄OsAs: C, 46.6; H, 4.74; As, 10.4. Found: C, 46.7; H, 4.82; As, 10.2. ¹H NMR (CD₂Cl₂): δ 7.53 (m, *m* + *p*-CH, 9H), 7.39 (m, *o*-CH, 6H), 2.13 (s, C₅Me₅, 15H), -9.88 (s, Os-H, 4H). ¹³C{¹H} NMR (CD₂Cl₂): 132.6 (s, *i*-C), 132.2 (s, *o*-C), 132.0 (s, *p*-C), 129.9 (s, *m*-C), 99.6 (s, C₅Me₅), 11.1 (s, C₅Me₅). IR (Nujol, cm⁻¹): 2088 (w), 2029 (w), 1568 (w), 1563 (w), 1476 (m,sh), 1439 (s), 1420 (w), 1366 (m, sh), 1340 (w), 1313 (w), 1307 (w), 1281 (w), 1184 (w), 1166 (w), 1151 (w), 1096 (m), 1081 (s), 1054 (s), 1035 (s), 999 (m), 988 (w), 977 (w), 971 (w), 961 (w), 933 (w), 911 (w), 865 (w), 848 (w), 833 (w), 807 (w), 795 (w), 754 (s), 748 (s), 723 (w), 702 (w), 694 (m), 668 (w), 634 (w), 613 (w), 576 (w), 522 (w), 486 (w), 475 (m), 460 (w), 416 (w), 407 (w).

(Pentamethylcyclopentadienyl)dihydrido(η²-dihydrogen)(tricyclohexylphosphine)osmium(IV) Tetrafluoroborate, [(C₅Me₅)Os(PCy₃)H₂(H₂)] [BF₄] (3). To a solution of (C₅Me₅)OsH₃(PCy₃) (0.15 g, 0.25 mmol) in diethyl ether (10 mL) was added HBF₄·Et₂O (0.15 mL, 2.0 mmol). A white precipitate formed immediately. The solution was stirred at room temperature for 30 min, and the white solid was collected by filtration. Yield: 0.09 g (52%). Anal. Calcd for C₂₈H₅₂BF₄OsP: C, 48.3; H, 7.52; P, 4.45. Found: C, 48.5; H, 7.98; P, 4.27. ¹H NMR (CD₂Cl₂): δ 2.27 (s, C₅Me₅, 15H), 1.90 (m, PCy₃, 6H), 1.76 (m, PCy₃, 9H), 1.68 (m, PCy₃, 3H), 1.27 (m, PCy₃, 15H), -10.61 (d, J_{PH} = 15.7 Hz, Os-H, 4H). ¹³C{¹H} NMR (CD₂Cl₂): δ 99.8 (s, C₅Me₅), 38.7 (d, J_{PC} = 30.4 Hz, 1-C), 29.8 (d, J_{PC} = 2.8 Hz, 3-C), 27.5 (d, J_{PC} = 12.0 Hz, 2-C), 26.5 (s, 4-C), 11.5 (s, C₅Me₅). ³¹P{¹H} NMR (CD₂Cl₂): δ 31.3 (s). IR (Nujol, cm⁻¹): 2173 (w), 2102 (w), 1423 (w), 1366 (w), 1348 (w), 1343 (w), 1329 (w), 1321 (w), 1306 (w), 1298 (w), 1279 (w), 1265 (w), 1226 (w), 1199 (w), 1185 (w), 1174 (m), 1127 (w), 1102 (m), 1086 (s), 1060 (s), 1047 (s), 1032 (s), 960 (w), 900 (w), 889 (w), 852 (w), 846 (w), 827 (w), 813 (m), 798 (w), 740 (w), 722 (w), 531 (w), 517 (w), 490 (w).

Crystallographic Studies.⁴² Single crystals of [(C₅Me₅)Os-(PPh₃)H₂(H₂)] [BF₄] (1), grown from 1:1 CH₂Cl₂/Et₂O, were mounted on glass fibers with Paratone-N oil (Exxon) and immediately cooled to -75 °C in a cold nitrogen gas stream on the diffractometer. [Single crystals of [(C₅Me₅)Os(PCy₃)H₂(H₂)] [BF₄] (3), grown from CH₂Cl₂/Et₂O, were treated similarly. Subsequent comments in brackets will refer to this compound.] The cell dimensions in Table 1 were calculated from 8192 [7099] reflections.

Data were collected with an area detector by using the measurement parameters listed in Table 1. The measured intensities were reduced to structure factor amplitudes and their esd's by correction for background, scan speed, Lorentz, and polarization effects. Systematic absences for *h*0*l* (*l* ≠ 2*n*) and 0*k*0 (*k* ≠ 2*n*) were only consistent with space group P2₁/c. [For 3, the cell constants were only consistent with space groups P1 and P1̄ and refinement was successful in the latter space group.] An empirical absorption correction was applied, the maximum and minimum transmission factors being 0.989 and 0.607. Systematically absent reflections were deleted, and symmetry-equivalent reflections were averaged to yield the set of unique data. Five reflections (11,16,2, -8,11,6, -12,13,1, 0,2,10, and -10,19,6) with F_o² < -3σ(F_o²) were suppressed. [For 3, a face-indexed absorption correction was applied, the maximum and minimum transmission factors being 0.844 and 0.529. The 0,0,1 reflection was obscured by the beam stop and was deleted.] The remaining 6463 [6629] data were used in the least-squares refinement.

The correct positions for the osmium and phosphorus atoms were deduced from a sharpened Patterson map. The quantity minimized by the least-squares program was Σw(F_o² - F_c²)² where w = {[σ(F_o²)]² + (0.0166P)² + 13.017P}⁻¹ and P = (F_o² + 2F_c²)/3 [for 3, w = {[σ(F_o²)]² + 7.0947P}⁻¹]. The analytical approxima-

(35) Luo, X. L.; Crabtree, R. H. *J. Am. Chem. Soc.* **1990**, *112*, 6912–6918.

(36) Gusev, D. G.; Nietlispach, D.; Eremenko, I. L.; Berke, H. *Inorg. Chem.* **1993**, *32*, 3628–3636.

(37) Gusev, D. G.; Berke, H. *Chem. Ber.* **1996**, *129*, 1143–1155.

(38) Lin, Z. Y.; Hall, M. B. *J. Am. Chem. Soc.* **1994**, *116*, 4446–4448.

(39) Gusev, D. G. *Organometallics* **2003**, *22*, 5148–5151.

(40) Gusev, D. G.; Hubener, R.; Burger, P.; Orama, O.; Berke, H. *J. Am. Chem. Soc.* **1997**, *119*, 3716–3731.

(41) Li, J.; Dickson, R. M.; Ziegler, T. *J. Am. Chem. Soc.* **1995**, *117*, 11482–11487.

(42) For a description of the crystallographic programs and procedures used, see: Brumaghim, J. L.; Priepot, J. G.; Girolami, G. S. *Organometallics* **1999**, *18*, 3139–2144.

tions to the scattering factors were used, and all structure factors were corrected for both real and imaginary components of anomalous dispersion. Independent anisotropic displacement factors were refined for the non-hydrogen atoms. Hydrogen atoms on the phosphine and C_5Me_5 ligands were placed in idealized tetrahedral locations with C–H = 0.98 Å (methyl) and 1.00 Å (methine); the methyl groups were treated as rigid rotators, and their positions were optimized by rotation about the C–C bond. The displacement parameters for the methyl hydrogen atoms were set equal to 1.5 times U_{eq} for the attached carbon atom, and the displacement parameters for the methine hydrogen atoms were set equal to 1.2 times U_{eq} . The osmium-bound hydrogen atoms were located in the difference Fourier maps, and their locations were independently refined with a common isotropic displacement factor. Convergence of the hydride locations was slow, especially for H4, and thus some doubt must be associated with their positions. [For **3**, methyl and methine hydrogens were treated as above; methylene hydrogens were placed in idealized positions with C–H = 0.99 Å and displacement parameters set equal to 1.2 times U_{eq} for the attached carbon atom. Likely positions for the osmium-bound hydrogen atoms surfaced in the latter stages of the refinement, and their positions were refined independently, except that a common displacement parameter was assigned for them.] An isotropic extinction parameter was refined to a final value of $x = 1.0(1) \times 10^{-6}$ [$2.5(2) \times 10^{-6}$], where F_c is multiplied by the factor $k[1 +$

$F_c^2 \lambda^3 / \sin 2\theta]^{-1/4}$ with k being the overall scale factor. Successful convergence was indicated by the maximum shift/error of 0.002 [0.001] for the last cycle. Final refinement parameters are given in Table 1. The largest peak in the final Fourier difference map ($2.29 e \text{ \AA}^{-3}$) was located 3.17 Å from the boron atom and 2.18 Å from F(4). [For **3**, the largest peak in the final Fourier difference map ($0.94 e \text{ \AA}^{-3}$) was located 1.18 Å from osmium.] A final analysis of variance between observed and calculated structure factors showed no apparent errors.

Acknowledgment. We thank the National Science Foundation (Grant Nos. CHE 00-76061 and CHE 04-20768) for support of this work, and Dr. Scott Wilson and Ms. Teresa Prussak-Wieckowska of the University of Illinois Materials Chemistry Laboratory for collecting the crystallographic data for **1** and **3**. C.L.G. thanks the University of Illinois at Urbana–Champaign for a departmental fellowship. We thank a reviewer for valuable comments about the interpretations of the solution NMR data.

Supporting Information Available: CIF files giving X-ray crystallographic data for $[(C_5Me_5)Os(PPh_3)H_2(H_2)][BF_4]$ (**1**) and $[(C_5Me_5)Os(PCy_3)H_2(H_2)][BF_4]$ (**3**). This material is available free of charge via the Internet at <http://pubs.acs.org>.

OM061017E